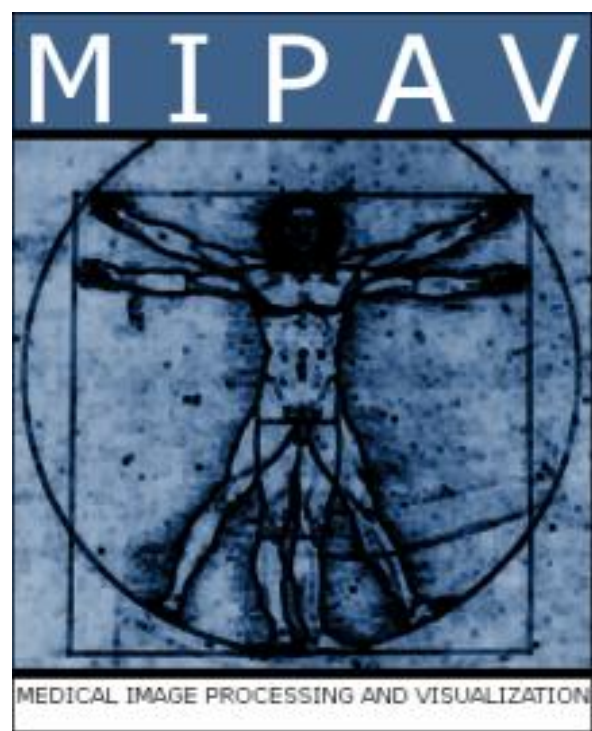


Tumor Treatment Response Identification Using Combination Post-Treatment Mapping to Quantify Voxel-Wise Multiparameter MRI Biomarker Changes: A Simulation Study



Justin Senseney**, David Thomasson, Ph.D.***, Robert Somer, M.D. †, Jyothi Jagannathan, M.D. ‡, Katherine Zukotynski, M.D.‡, Moira Schieke, M.D.‡

**Imaging Sciences Lab, Center for Information Technology, National Institutes of Health, Bethesda, MD.
 *** National Institute of Allergy and Infectious Disease, National Institutes of Health, Bethesda, MD.
 † Department of Hematology and Oncology, University of Medicine and Dentistry of New Jersey, NJ.
 ‡ Department of Radiology, Dana Farber Cancer Institute, Boston, M.A.



DANA-FARBER
CANCER INSTITUTE

Introduction

Simultaneous use of multiple MRI biomarkers from multiparameter MRI datasets could enhance MRI detection of early tumor treatment responses. Post-treatment mapping utilizes affine registration of the post-treatment MRI images with the pre-treatment MRI images to assess voxel-per-voxel tumor changes. Multiple clinical studies have shown voxel-wise post-treatment mapping for increases in ADC values (ADC+) shortly after Avastin treatment can stratify for differences in overall survival in glioma patients.^{1,2} Given this success, expanding parameter mapping strategies to include “combinations” of MRI biomarkers may be possible.

Multiple MRI measures show promise as potential tumor biomarkers and include Ktrns values from Dynamic Contrast-Enhanced MRI (DCE-MRI), ADC values from Diffusion-Weighted MRI (DWI-MRI), and R* values from Intrinsic-Susceptibility MRI (IS-MRI). Sources of error in MRI measurements, however, continue to be a substantial obstacle to more widespread use of these techniques. In particular, partial volume errors are a large source of error in MRI measures. Partial volume errors from MRI tumor tissue measurements occur within voxels at the edges of the tumor and within necrotic regions, resulting from inclusion of only a small portion of tumor within the voxel volume. The success of post-treatment mapping strategies in clinical studies may in large part be attributable to reduced partial volume errors. Therefore, we hypothesize that combining multiple MRI biomarkers into “combination” maps may improve accuracy of parameter measures by reducing partial volume errors, as well as improve the specificity of voxel-wise tissue characterization of tumor responses following treatment.

Here, we use customized software to analyze a “combination” voxel-wise post-treatment mapping strategy using simulations of growing and shrinking tumors with pre- and post-treatment parameter values matching tumor responses seen in clinical studies (decreased Ktrns-, increased ADC+, and increased R*+) (Figure 1).

MRI Biomarkers

Dynamic Contrast-Enhanced MRI (DCE-MRI), Intrinsic-Susceptibility MRI (IS-MRI), and Diffusion-Weighted Imaging (DWI) are tools for preclinical and clinical oncologic imaging. Varying levels of evidence exist to support the use of these techniques as MRI Biomarkers for tumor responses to treatment.

Dynamic Contrast-Enhanced MRI (DCE-MRI)

Tumor vessels are larger, more leaky, and more tortuous than normal vessels, and DCE-MRI provides a tool to measure indices of this variant vasculature.

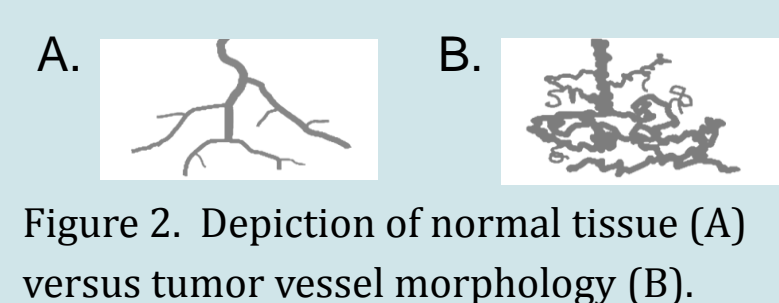
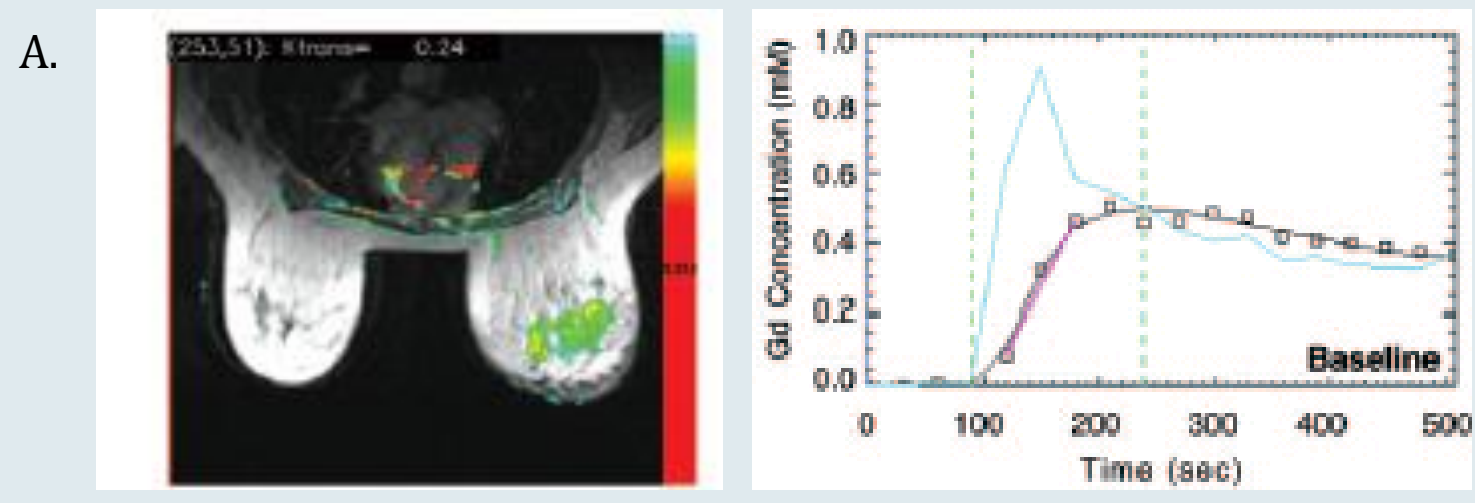


Figure 2. Depiction of normal tissue (A) versus tumor vessel morphology (B).

DCE-MRI uses dynamic imaging (repeat scanning over multiple time points) and pharmacokinetic modeling. A region of interest (ROI) is used to measure a vascular input function (VIF) and tissue contrast concentration per time (C_t(t)).



K^{trns}	Forward Exchange Constant	Figure 3.
k_{ep}	Reverse Exchange Constant	
f_{bv}	Fractional Blood Volume	
v_e	Volume of Exchange	

Pharmacokinetic parameters are determined using VIF and tissues curves as fitting input. Parameters generated using a computer program that have been validated in animal studies³ uses the “General Kinetic Model” (GKM) and a direct convolution of the VIF to tissue curves according to:

$$C_t(t) = \frac{1-f_{bv}}{1-Hct} K^{trns} \left[C_b(t) \otimes e^{-\frac{K^{trns}}{v_e} t} \right] + f_{bv} C_b(t)$$

Ktrns, the forward exchange rate constant, is the parameter predominantly used in clinical trials. Numerous studies showing stratification for overall survival in cancer patients using Ktrns early after treatment provide strong support for the use of DCE-MRI as an MRI biomarker. DCE-MRI has been included in recently updated tumor response criteria, RECIST 1.1.⁴

Diffusion-Weighted MRI (DWI-MRI)

DWI-MRI uses gradients of various weights, or “b-values,” to measure indices of the Brownian motion of water molecules. Tumors have “restricted diffusion” and maintain signal on higher b-value DWI-MRI images. The Apparent Diffusion Coefficient (ADC) is a measure of the slope of signal values at various b-values and are thus lower in tumors.

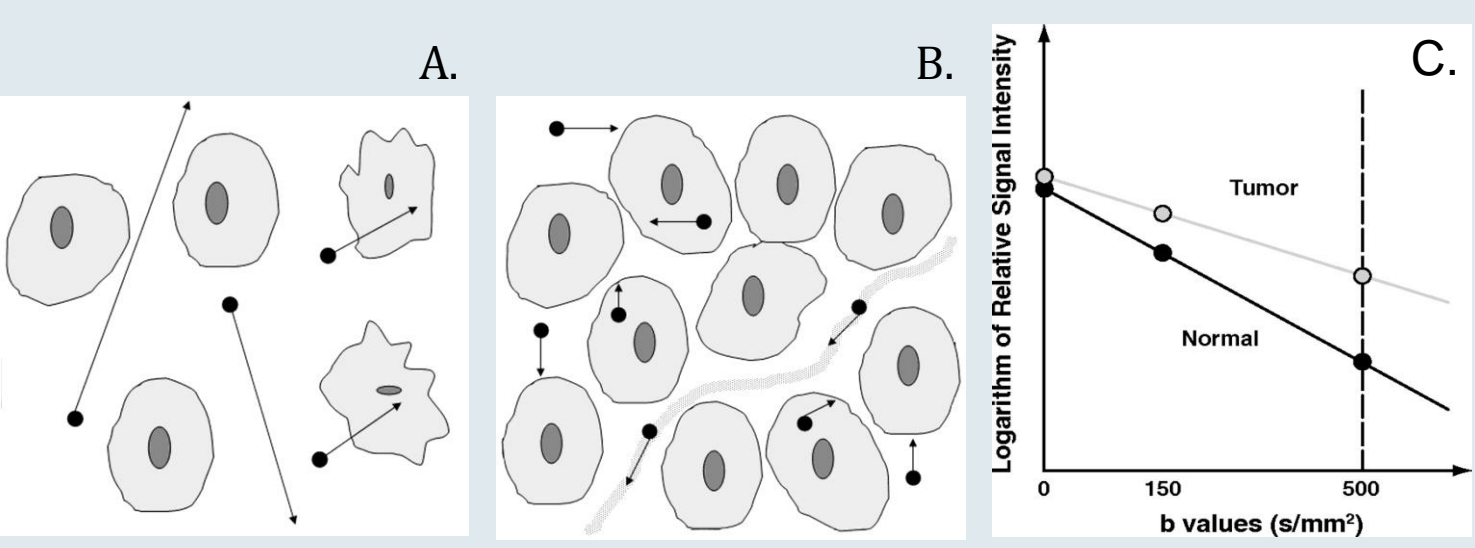


Figure 4. Depiction of Brownian motion of water in normal tissues (A) versus tumor (B). ADC values equal the slope of the log (signal) versus b-values (C).⁵

Strong evidence supports the use of DWI-MRI as a biomarker for tumor responses.⁶

Intrinsic Susceptibility MRI (IS-MRI)

R* determined from IS-MRI are indices of hypoxia. In prostate cancer, for example, R* measures have been shown to have high sensitivity, although low specificity, to intra-prostatic tumor hypoxia.⁷ Currently, insufficient evidence exists to support the use of R* measures MRI biomarkers of tumor responses.

Combination Parameter Mapping

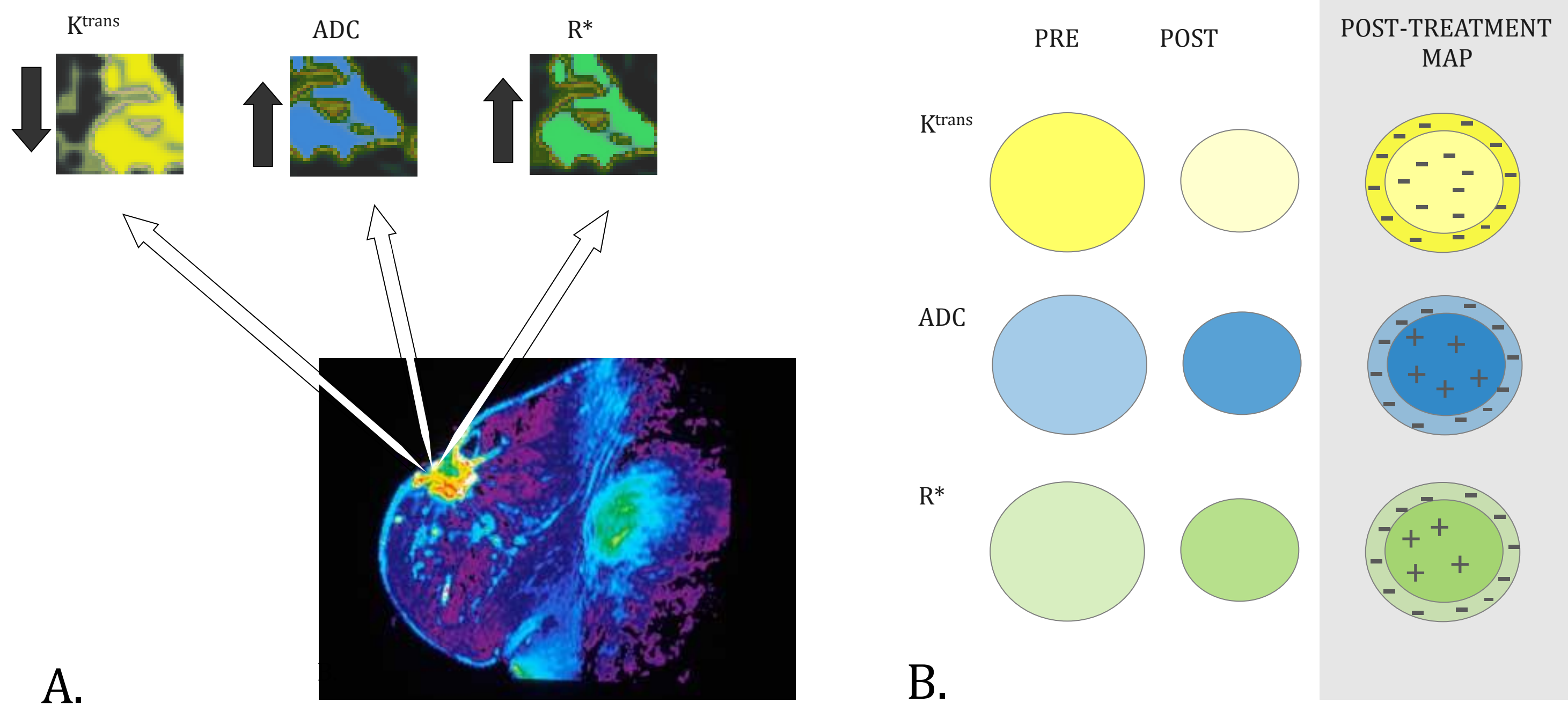


Figure 1. Schematic diagram demonstrates the concept of “combination” parameter mapping. (A) In theory, registered multiparameter MRI images of pre- and post-treatment tumor could provide high resolution data of voxel-wise and simultaneous changes in multiple different MRI biomarkers. In this hypothetical case of a single voxel in a breast cancer, parameter changes for Ktrns, ADC, and R* after treatment all followed expected tumor response changes as demonstrated in published literature. ADC and R* values have been shown to increase following treatment (ADC+, R*+), while Ktrns values have been shown to decrease (Ktrns-). (B) When parameter values increase but tumor size decreases, post-treatment parameter maps will contain central areas of ADC+ or R*+, but peripheral areas of ADC- and R*-. Conversely, when a parameter value decreases and tumor size decreases, all values in the post-treatment map are decreased. Selection of combined ADC+ / R*+ / Ktrns- includes voxels within central regions of tumor and omits regions at the periphery which contain the highest proportion of partial volume errors.

Methods

Computer-Generated MRI Tumor Models Simulated tumors (n=25) were generated using MIPAV software. (<http://mipav.cit.nih.gov>) (MIPAV version 5.4.2, CIT, NIH, Bethesda, M.D.)⁸ “True tumors” were generated using MIPAV image creation and image sculpting capabilities ranging from 6 cm in diameter to 0.4 cm. Each voxel value in the tumor was initially set to “1” and voxels surrounding the tumor were set to “0.” “True tumor” isotropic images had a resolution 0.117mm. “MRI tumors” were subsequently created using an algorithm to model partial volume effects. Partial volume effects were simulated using subsampling of “true tumor” images to generate a Gaussian weighted average of 26 neighboring pixels which was then displayed as simulated MRI acquisitions with a voxel resolution of 2mm. For Ktrns values, each voxel with partial voluming was additionally multiplied by a factor of 0.33 to model nonlinear partial volume effects seen for Ktrns values in a validation study.³ Each voxel in the “MRI tumor” volumes was then multiplied by a desired tumor “pre-” or “post-treatment” parameter value based on published literature. Pre-treatment and post-treatment values were as follows: Ktrns = 0.10 pre, 0.066 post,⁹ ADC = 0.00109 pre, 0.00201 post,¹⁰ and R* = 31.7 pre, 36.5 post.¹¹

Post-Treatment Parameter Maps A plug-in created for MIPAV software was used to generate post-treatment parameter maps and output desired measures and statistics. Post-treatment parameter maps were created by subtracting the pre-treatment MRI tumor volume from the post-treatment MRI tumor volume for each combination of “MRI tumors” representing various changes in volume of pre- and post-treatment tumors ranging between an increase in size of 54% to a decrease in size of 54%. Percent of partial voluming in each post-treatment map was determined.

MRI Tumor Model Measures and Percent Error Analysis Changes in parameter measurements for pre- and post-treatment “MRI tumor” models was determined for both hand-drawn regions of interest (HD-ROI) and for voxel-wise values from post-treatment parameter maps. For the hand-drawn ROI, the MIPAV ROI tool was used to manually draw an ROI around the tumor edges on a central slice of both the pre- and post-treatment “MRI tumors” and determine the average voxel value for each. For each tumor, the ROI for the post-treatment tumor was generated by manually drawing a second ROI (HD-ROI, type 1) or by copying the pre-treatment ROI onto the post-treatment “MRI tumor” (HD-ROI, type 2). The change in parameter value was determined by subtracting the pre-treatment measure from the post-treatment measure. Three sets of values were generated for each post-treatment parameter map. In cases when the parameter values increased but the tumor size decreased, resultant parameter maps contained central positive voxel values and peripheral negative voxel values. Similarly, in cases when the parameter value decreased and tumor size increased, resultant parameter maps contained central negative values and peripheral positive values. In cases where the parameter value decreased as the tumor size decreased, or vice versa, the resultant maps contained only negative or positive values, respectively. The average voxel value was determined for all tumor voxels (ADC+, R*+, and Ktrns+), voxels with positive values (ADC+, R*+, and Ktrns+), and voxels with negative values (ADC-, R*-, and Ktrns-). The percent error was determined as the percent difference between the measured values and the expected “true” measures.

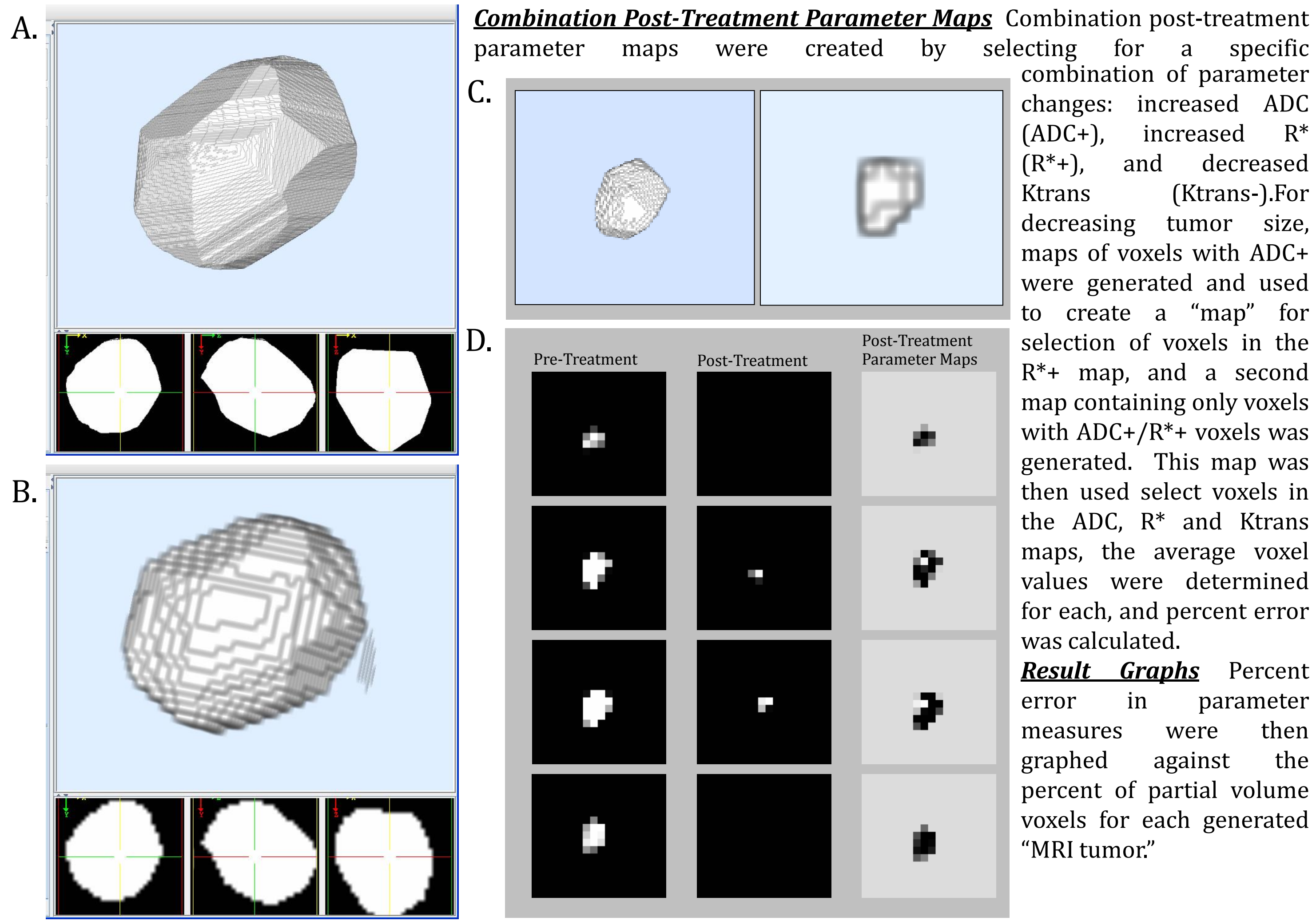


Figure 5. MIPAV software generated tumor models and post-treatment parameter maps. (A) Example “true tumor” measuring approximately 6cm at greatest diameter and the corresponding “MRI tumor” (B). Example smaller tumors (C) showing the increased proportion of partial volume voxels in the “MRI tumor” (b) as compared to the “true tumor” (a). Example post-treatment parameter maps for R* (D) in a small tumor with original diameter of approximately 8mm, pre-treatment “true tumor” voxel values of 31.7, post-treatment values of 36.5, and a decrease in size after treatment. Maps were generated by subtracting the pre-treatment “MRI tumor” slice from the corresponding post-treatment “MRI tumor” slice. Images demonstrate the large proportion of partial volume effects in the small tumor. All tumor voxels in the “true tumor” have the same values and white voxels contain “true” values, while voxels with shades of grey contain partial volume errors. Post-treatment maps show the expected stratification into R*+ and R*- voxels.

Results

Post-Treatment Parameter Mapping for ADC+, R*+, and Ktrns- Results show individual parameter mapping for Ktrns- with increasing tumor size and ADC+, or R*+ with decreasing tumor size significantly decreased percent error from “true” values compared to hand-drawn ROI and total parameter map values. Tumor sizes ranged from 6 cm to 0.4 cm in diameter, and the smallest tumors had the highest proportion of partial voluming. In each case, discarded voxels had a high percent partial volume error and percent error.

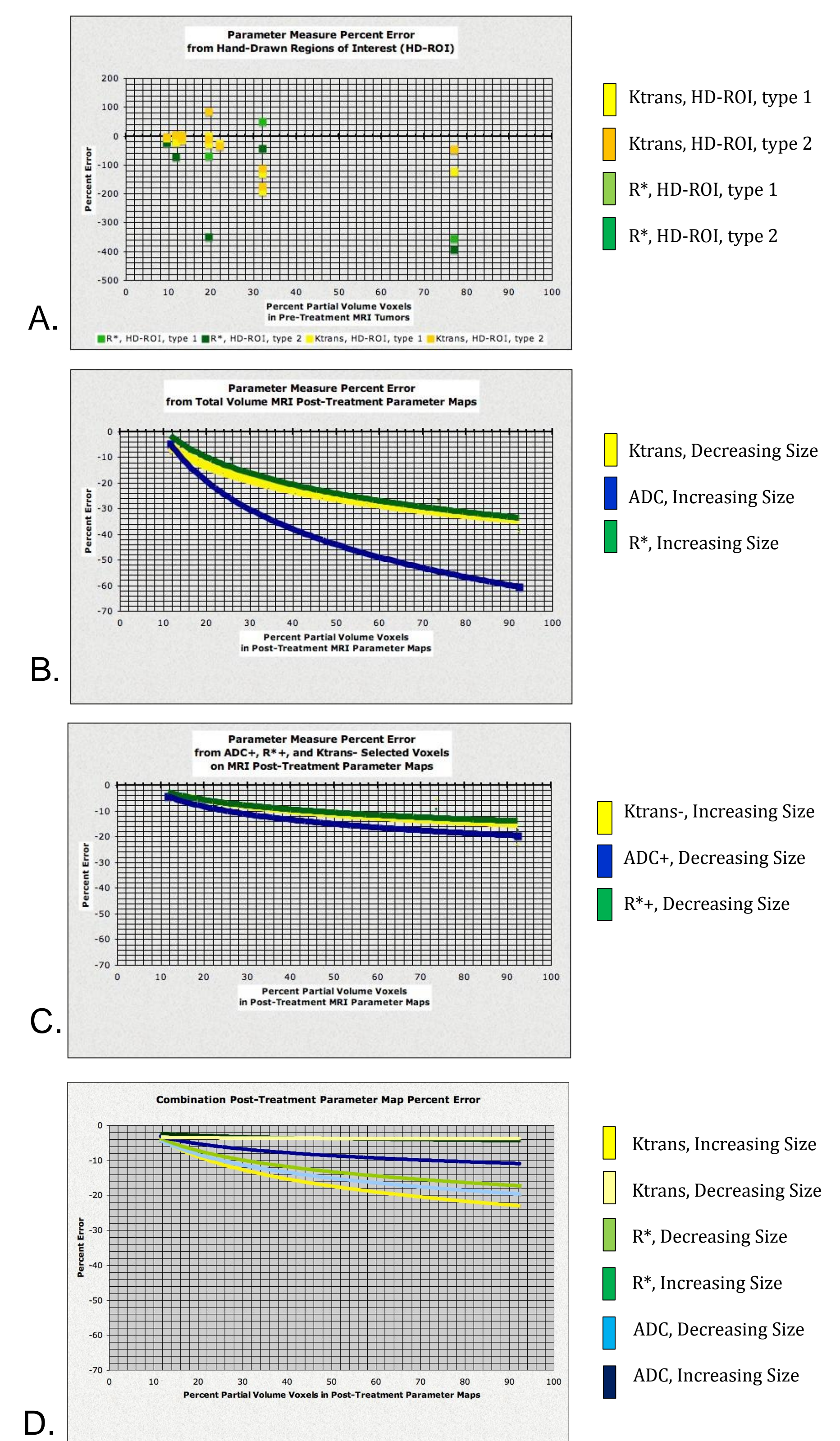


Figure 6. (A) HD-ROI: Percent error varied randomly with percent partial voluming, increasing up to 400%. (B) Total Parameter Map Values: Percent error increased logarithmically versus percent partial voluming with decreasing tumor size (Ktrns-: -8.0% to -38.7% and increasing tumor size for ADC and R* (R*error: -4.6% to -60.5% and -4.4% to -38.3%). (C) ADC+, R*+, Ktrns-: Percent error improved for ADC+ and R*+ with decreasing tumor size (Ktrns-: -4.2% to -19.6% and -3.6% to -17.2%). Percent error improved for Ktrns- with increasing tumor size (Ktrns-: -3.9% to -22.9%). (D) Combined Ktrns- / ADC+ / R*+: Selection of voxels for Ktrns- / ADC+ / R*+ improved percent error for increasing tumor size (Ktrns-: -3.9% to -22.9%, ADC: -3.2% to -10.9%, R*+: -2.2% to -4.3%) and decreasing tumor size (Ktrns-: -3.3% to -4.2%, ADC: -4.2% to -19.6%, R*+: -3.6% to -17.2%).

Combination Post-Treatment Parameter Mapping Selection of voxels with specific combinations of parameter changes (Ktrns-, ADC+, and R*+) resulted in further decreases in percent error. Results demonstrate that combination parameter mapping helps discard voxels with a high proportion of partial volume error, thus leading to improved percent error. Assuming adequate registration and low MRI noise, results suggest combination parameter mapping would possibly be able to detect changes in very small tumors with diameters on the order of only a few millimeters.

Conclusions and Future Work

Simulations using computer-generated tumors proved an effective tool for analysis of a novel concept in assessment of MRI measurement of tumor responses. These simulations show that “combination” post-treatment mapping is a promising strategy to decrease partial volume errors and increase MRI detection of early tumor treatment responses.

Future work is focused on improving the simulations to better model real data. For example, MRI noise profiles will be included in a future MIPAV plug-in simulation tool. In addition, a second MIPAV plug-in will be used to generate Combination Parameter Maps on real data from cancer patients undergoing treatment.

References

- Galbán CJ, Chenevert TL, Meyer CR, Tsien C, Lawrence TS, Hamstra DA, Junck L, Sundgren PC, Johnson TD, Ross DJ, Reheultulla A, Ross BD. The parametric response map is an imaging biomarker for early cancer treatment outcome. *Nat Med.* 2009 May;15(5):572-6.
- Ellingson BM, Cloughesy TF, Lai A, Mischak PS, Nghiemphu PL, Lalezari S, Schmandt KM, Pope WB. Graded functional diffusion map-defined characteristics of apparent diffusion coefficients predict overall survival in recurrent glioblastoma treated with bevacizumab. *Neuro Oncol.* 2011 Oct;13(10):1151-61.
- Ferreir MC, Sarin H, Fung SH, Schatto B, Pluta RM, Gupta SN, Choyke PL, Oldfield EH, Thomasson D, Butman JA. Validation of dynamic contrast-enhanced magnetic resonance imaging-derived vascular permeability measurements using quantitative autoradiography in the RG2 rat brain tumor model. *Neoplasia.* 2007 Jul;9(7):546-55.
- Nishino M, Jagannathan JP, Ramaiya NH, Van den Abbeele AD. Revised RECIST guideline version 1.1: What oncologists want to know and what radiologists need to know. *AJR Am J Roentgenol.* 2010 Aug;195(2):281-9.
- Koh DM, Collins DJ. Diffusion-weighted MRI in the body: applications and challenges in oncology. *AJR Am J Roentgenol.* 2007 Jun;188(6):1622-35.
- Padhani AR, Liu G, Koh DM, Chenevert TL, Thoeny HC, Takahara T, Driz-Jurasz A, Ross BD, Van Cauteren M, Collins D, Hammond DA, Rustin GJ, Taouli B, Choyke PL. Diffusion-weighted magnetic resonance imaging as a cancer biomarker: consensus and recommendations. *Neoplasia.* 2009 Feb;11(2):102-25.
- Hoskin PJ, Carrell DM, Taylor NJ, Smith RE, Stirling JJ, Daley FM, Saunders MI, Bentzen SM, Collins DJ, d'Arcy JA, Padhani AP. Hypoxia in prostate cancer: correlation of BOLD-MRI with pimonidazole immunohistochemistry-initial observations. *Int J Radiat Oncol Biol Phys.* 2007 Jul;68(4):1065-71.
- M. J. McAuliffe, F. M. Lalonde, D. McGarry, W. Gandler, K. Csaky, and B. L. Trus, “Medical Image Processing, Analysis and Visualization in clinical research,” in *Computer-Based Medical Systems, 2001. CBMS 2001. Proceedings. 14th IEEE Symposium on*, 2001, pp. 381–386.
- Wedam SB, Low JA, Yang SK, Chow CK, Choyke P, Danforth D, Hewitt SM, Bertram A, Steinberg SM, Liewehr DJ, Plehn J, Doshi A, Thomasson D, McCarthy N, Koopman H, Sherman M, Zujewski J, Campbell K, Chen H, Swain SM. Antiangiogenic and antitumor effects of bevacizumab in patients with inflammatory and locally advanced breast cancer. *J Clin Oncol.* 2006 Feb 10;24(5):769-77.
- Hayashida Y, Yakushiji T, Arai K, Katahira K, Nakayama Y, Shimomura O, Kitajima M, Hirai T, Yamashita Y, Mizuta H. Monitoring therapeutic responses of primary bone tumors by diffusion-weighted imaging: Initial results. *Eur Radiol.* 2006 Dec;16(12):2637-43.
- L. S.P. Taylor, N. Makris, A. Ah-Sue ML, Beresford MJ, Stirling JJ, d'Arcy JA, Collins DJ, Padhani AR. Primary human breast adenocarcinoma: imaging and histologic correlates of intrinsic susceptibility-weighted MRI imaging before and during chemotherapy. *Radiology.* 2010 Dec;257(3):643-52.